

Argon retentivity and argon excess in amphiboles from the garbenschists of the Western Tauern Window, Eastern Alps

F.v. Blanckenburg¹ and I.M. Villa²

¹ Institut für Kristallographie und Petrographie, ETH-Zentrum, CH-8092 Zürich, Switzerland

² Istituto di geocronologia e geochimica isotopica, CNR, Via Cardinale Maffi 36, I-56100 Pisa, Italy

Abstract. 22 hornblende K-Ar ages and 10 ³⁹Ar–⁴⁰Ar spectra were obtained for hornblende garbenschists from the Western Tauern Window. The post-kinematic amphiboles were produced during the late Alpine prograde metamorphism (6–10 kb and 500–570° C). Two nearly potassium-free cummingtonites rimming hornblende yield K-Ar ages of 120 Ma, while the 20 tschermakitic hornblendes scatter between 17 and 37 Ma. The reason for this scatter is excess Ar, possibly incorporated into amphiboles during healing of fractures, now traceable by trails of fluid inclusions. Excess Ar is semiquantitatively corrected for by combining cogenetic hornblende and cummingtonite with K-Ar isochrons. It can be quantified in 4 out of 10 hornblendes by ³⁹Ar–⁴⁰Ar stepwise heating experiments. Ages of 18–20 Ma result for corrected hornblendes. The retentivity of ⁴⁰Ar, after correction for excess, shows no correlation with chemistry within the narrow compositional range observed; rather, it shows intriguing correlations with irregularities in Ca/K spectra, pointing to a microstructurally controlled mechanism for Ar loss. This observation leads to a critical evaluation of the closure temperature “constant”, which apparently depends on an incompletely known number of mineralogical and environmental parameters. In particular those ³⁹Ar–⁴⁰Ar release spectra which yield low temperature steps with younger ages than the plateaus are not interpretable in terms of a synchronous closure. This gives evidence that loss of radiogenic isotopes proceeds by a more complex mechanism than simple volume diffusion through isotropic media.

Introduction

During recent years the significance of amphibole argon dating for the geochronometry of metabasic regional metamorphic rocks has been increasingly recognized. The usually observed high argon-retentivity of amphiboles suggests that, besides white mica Rb-Sr, the hornblende K-Ar system may be the most appropriate for dating (1) the crystallization of metamorphic mineral assemblages or (2) closure at a high temperature (Hanson and Gast 1967; Harrison 1981). However, there is no unanimous interpretation of amphibole K-Ar ages.

Several authors have used hornblende age data to demonstrate the effects of mineral chemistry on argon retentivity, while others argued principally against the blocking temperature concept. A clear case of mineral chemistry-dependent argon retentivity was shown by Harrison and Fitz Gerald (1986) on the basis of an Ar-Ar release spectrum of metamorphic hornblende containing exsolution lamellae of cummingtonite, the latter exhibiting significantly lower ages than hornblende. O’Nions et al. (1969) show a dependency of Ar-retentivity and the Fe/Mg-ratio in hornblende. Berry and McDougall (1986) observed preferred resetting of Fe-rich hornblendes at upper greenschist and lower amphibole facies conditions, while Mg-rich hornblendes partly retain their radiogenic Ar. Hornblende K-Ar data from the Central Alps (Steiger 1964; Deutsch and Steiger 1985) have been used to argue against the application of the blocking temperature concept; they suggest that recrystallization subsequent to pervasive tectonic deformation is responsible for age resetting of hornblende rather than temperature controlled diffusional loss.

The significance of amphibole K-Ar ages is often obscured by the occurrence of unknown quantities of excess argon, i.e. nonatmospheric ⁴⁰Ar not deriving from in-situ decay of K contained in the mineral. Because amphiboles are low in K-content and hence poor in radiogenic Ar, they are quite sensitive to even small amounts of such excess Ar. Examples of excess Ar are well-known and first reviewed by Dalrymple and Lanphere (1969). ⁴⁰Ar–³⁹Ar spectra showing excess Ar in amphiboles are given by Harrison and McDougall (1980, 1981) and Villa (1983). The possible occurrence of excess Ar in Alpine amphiboles is discussed by Zeitler and Wijbrans (1986) and Deutsch and Steiger (1986). Conclusive interpretation of K-Ar data on hornblende appears to be possible only if adequate methods are found to single out the effects of excess Ar.

This study presents 20 hornblende and 2 cummingtonite K-Ar ages and 10 ³⁹Ar–⁴⁰Ar spectra on hornblendes. The interpretation mainly focuses on (1) excess Ar in amphiboles and (2) the question of Ar-retentivity in order to test the suitability of the K-Ar chronometer in amphiboles from regional metamorphic rocks. In a companion study, Blanckenburg and Morteani (1988) give petrographic details and chemical and phase petrological data on the studied amphibole samples. The regional geologic implications and new T calibrations in a pressure-temperature-time path are discussed elsewhere (Blanckenburg et al. 1988).

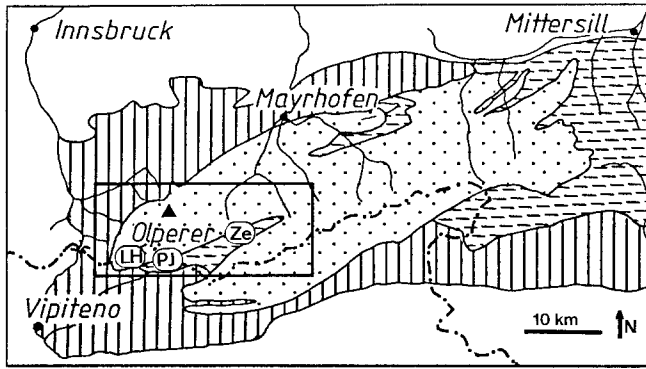


Fig. 1. Schematic geological map showing the sampling areas and sample numbers. *Ze* Oberer Zemmgrund, *PJ* Pfitscher Joch (Passo di Vizze), *LH* Landshuter Huette. *Dots* Zentralgneis, *vertically shaded* Obere Schieferhuelle, *dashed* Untere Schieferhuelle

Geological, petrographic, and geochronological framework

The Tauern Window in Western Austria and Northeast Italy is a tectonic window in which nappes of the Penninic basement terrain are exposed beneath Austroalpine thrust sheets (Fig. 1). The lower Schieferhuelle (LSH), in which the massive hornblende garbenschists occur, comprises an autochthonous post-Hercynian series of metasediments and amphibolites (Lammerer 1986), and the pre-Hercynian metasedimentary and metavolcanic country rock which was intruded by the Hercynian Zentralgneis complex. The metamorphic grade increases from greenschist to amphibolite facies towards the center of the window (Morteani 1974). Evidence for high pressure metamorphism in the garbenschists of the lower Schieferhuelle was found by Selverstone et al. (1984): mineral cores yielded initial pressures of about 10 kbars and temperatures of 530° C, whereas rims of minerals reflect the subsequent uplift and heating with a thermal climax at 6–7 kbar and 550° C. From these data a relatively complete PT-path was reconstructed.

K-Ar amphibole ages (Besang et al. 1968; Cliff et al. 1971; Raith et al. 1978) scatter irregularly between 597 and 21 Ma. A first ³⁹Ar–⁴⁰Ar release spectrum for a hornblende from the eastern Tauern Window (Cliff et al. 1985) was interpreted as dating the amphibole facies thermal climax at this deep structural level at 24 Ma.

Sample locations and descriptions

Three sampling locations were selected along an east-west traverse in the basement units of the Western Tauern Window (Fig. 1). Location Zemmgrund (Ze) and Pfitscher Joch (PJ) are located within the Lower Schieferhuelle which consists mainly of coarse-grained hornblende garbenschists. The maximum metamorphic temperatures are 570° C and 550° C, respectively. Location Landshuter Huette (LH) is a small garbenschist lens within the Paleozoic Zentralgneis complex. The peak metamorphic temperature is 500–540° C at LH. Petrographic details of the studied samples are given by Blanckenburg and Morteani (1988). They show that hornblende overgrew the dominant *s*₁ foliation during decompression and heating of the Alpine “Tauernkristallisation”. During the temperature maximum cummingtonite overgrowths formed at the rims of green hornblendes, e.g. Ze4 and Ze5, due to a *prograde* breakdown of chlorite (Fig. 2b). Amphibole growth was accompanied by *s*₂ microfracturing. These microfractures were later completely annealed in matrix minerals and partly in rims of amphiboles, but still traceable through trails of fluid inclusions. Large *s*₃ exten-

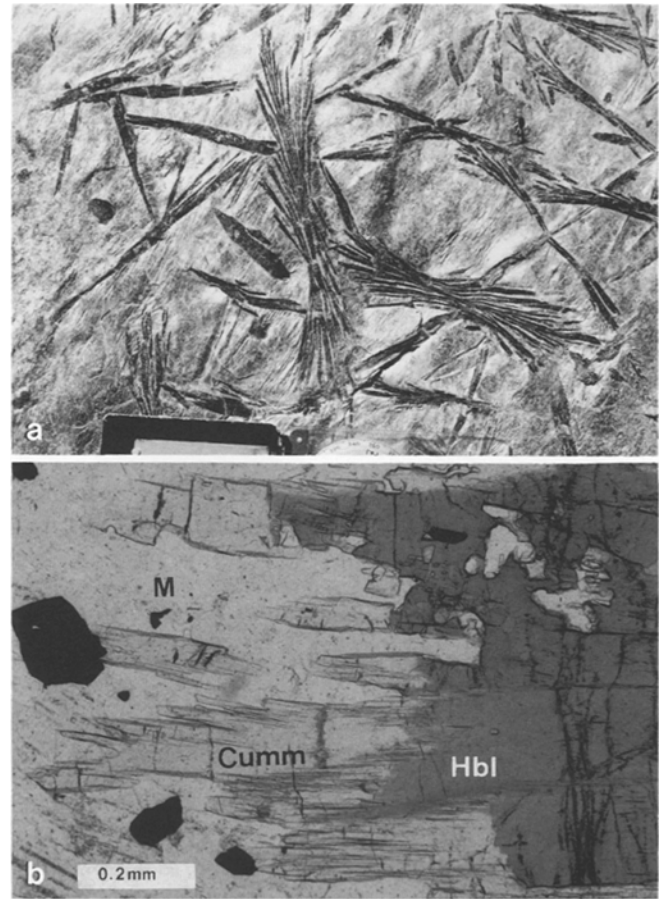


Fig. 2. **a** Handspecimen showing porphyroblastic hornblende “sheaves”. Note tensional cracks; **b** Photomicrograph showing green hornblende (*Hbl*) overgrown by colorless cummingtonite (*Cumm*). Both amphiboles are cracked. The microcracks are missing in the matrix (*M*) formed by quartz

sional cracks visible to the naked eye (Fig. 2a) crosscut *s*₂ microcracks and are filled with the mineral assemblage of the temperature maximum. Microprobe analyses of all dated amphiboles are given by Blanckenburg and Morteani (1988). All hornblendes are tschermakites with total alumina close to the maximum and a narrow overall compositional range. Only Fe²⁺/Mg scatters considerably.

Age determinations and results

Sample-preparation and analytical methods

After structural analysis and examination of the microfabric a part of each sample selected for dating was crushed and minerals separated using standard techniques. Heavy liquids were used only on sample PJ3. Intergrowths and dust were removed by use of an ultrasonic disintegrator in ethanol bath and the product hand-picked twice in order to guarantee a final purity exceeding 99%. Residual inclusions were mainly quartz and ilmenite. New separates were handpicked later from different magnetic fractions for ³⁹Ar–⁴⁰Ar measurements. Special procedures were used for structurally oriented minerals, which were carved off the handspecimen. Cummingtonite overgrowths on hornblende prisms were scratched off and then separated from hornblende by handpicking. For separating core and rim of large hornblende porphyroblasts, the sample was cut into 4 mm thick slices perpendicular to the *c*-axis of linear crystals. From these slices core and rim were excavated using a

Table 1. Amphibole K-Ar Results. Measurements marked with stars were used for Figs. 3 and 4 and further discussion

Sample number	Material	Grain size	K	³⁶ Ar	³⁸ Ar	⁴⁰ Ar	⁴⁰ Ar	Weight	Calculated age	
	Sampling-elevation [m]	[microns]	[ppm]	[in units 10 ⁻⁸ ccSTP/g]			[%Rad]	[mg]	[Ma]	
Zemmgrund										
Ze 2	HBL	1800	75-180	2710.0	0.532	0.0995	177.0	11	16.2	18.8 ± 3.4
Ze 2	HBL		75-180	2710.0	0.2033	0.03766	80.7	26	46.8	19.5 ± 1.6*
Ze 3I	HBL	1800	150-300	2890.0	0.1740	0.03284	72.6	29	78.4	18.8 ± 1.2*
Ze 3I	HBL		150-300	2890.0	0.1049	0.0098	52.83	41	28.1	19.3 ± 1.0
Ze 3III	HBL	1800	150-300	2920.0	0.1376	0.02557	61.1	34	93.4	17.9 ± 1.0*
Ze 4 Planar	HBL	1800	150-300	2300.0	0.1024	0.01922	46.33	35	95.4	17.9 ± 1.0*
Ze 4 Planar	HBL		150-300	2300.0	0.1165	0.0153	51.46	33	42.1	19.0 ± 1.2
Ze 4 Linear	HBL	1800	150-300	2640.0	0.794	0.1495	257.9	9	106.0	22.6 ± 4.6
Ze 4 Linear	HBL		150-300	2640.0	0.0742	0.0052	47.14	54	31.9	24.4 ± 1.0*
Ze 5 Core	HBL	1800	125-200	2330.0	0.0753	0.01390	40.61	45	37.1	20.1 ± 0.8*
Ze 5 Rim	HBL		125-200	2380.0	0.767	0.01445	41.07	45	39.3	19.8 ± 0.8*
Ze 9	HBL	2000	100-200	3200.0	0.388	0.0725	143.0	20	29.2	22.8 ± 2.2
Ze 9	HBL		100-200	3200.0	0.1693	0.03187	79.3	37	51.1	23.4 ± 1.2*
Ze 17	HBL	2400	125-180	3150.0	0.360	0.0671	136.4	22	26.7	24.4 ± 2.0
Ze 17	HBL		125-180	3150.0	0.1507	0.0278	75.1	41	37.4	24.8 ± 1.4*
Ze 19 Core	HBL	2500	150-320	2930.0	0.0553	0.1036	55.31	70	120.0	33.9 ± 1.2*
Ze 19 Rim	HBL		150-320	2880.0	0.0366	0.0041	43.11	75	93.5	28.6 ± 1.0*
Ze 20	HBL	2550	75-200	4220.0	1.274	0.2368	403.7	7	26.5	16.4 ± 4.6
Ze 20	HBL		75-200	4220.0	0.0931	0.01737	58.09	53	138.5	18.6 ± 0.8*
Ze 4 Cumm	CUMM	1800	125-500	165.0	0.2039	0.0382	68.1	11	29.6	118 ± 22.0*
Ze 5 Cumm	CUMM	1800	125-500	94.0	0.575	0.1083	174.5	3	67.6	120 ± 86.0*
Pfitscher Joch										
PJ 1	HBL	2640	150-300	3440	0.1495	0.0228	68.2	35	63.8	17.9 ± 1.0
PJ 1	HBL		150-300	3440	0.0699	0.01296	45.41	55	71.5	18.5 ± 0.6*
PJ 3	HBL	2570	200-350	2730	0.1230	0.0154	56.07	35	46.7	18.5 ± 1.0*
PJ 5	HBL	2200	125-200	3700	0.1690	0.0222	74.5	33	35.9	17.0 ± 1.0*
PJ 6	HBL	2300	200-350	2580	0.1121	0.0169	64.2	48	78.4	30.7 ± 1.2*
PJ 8	HBL	2400	125-250	3570	0.1407	0.02598	65.0	36	41.2	16.8 ± 1.0*
PJ 8	HBL		125-250	3570	0.453	0.0775	158.7	16	46.6	17.8 ± 2.0
Landshuter Hütte										
LH 1	HBL	2735	250-350	3680	0.2167	0.04039	112.4	43	59.7	35.5 ± 1.4*
LH 1	HBL		250-350	3680	0.378	0.0711	165.6	33	32.9	37.3 ± 2.0
LH 3	HBL	2735	180-250	3780	0.0633	0.01162	54.15	65	50.8	24.0 ± 0.8*
LH 6	HBL	2735	250-350	3330	0.1438	0.02772	81.7	48	42.1	30.1 ± 1.2
LH 6	HBL		250-350	3330	0.1335	0.02515	76.9	49	22.7	28.8 ± 1.2*

water cooled dentist's drill. The separates obtained by this method did not, of course, represent *pure* regions of core and rim in the crystal.

K concentrations were determined in Zurich by isotope dilution, using a K single spike; measurements were made partly on a tandem and on a Finnigan MAT 261 mass spectrometer. Mass spectrometer reproducibility for K was in the range of 0.6%. However, replicate K-analysis of hornblende-splits yielded 3% relative sample inhomogeneity (2 Sigma). This error has been propagated for age-error calculation.

Argon analyses were carried out on the Zürich all-metal on-line rare gas system. The spectrometer, using a GS 98 Baur-Signer source, operates with 3KV acceleration voltage, and a magnet with 120 mm radius and 90° angle of deflection. Concentrations are calibrated by measurement of extremely well-known quantities of purified atmospheric argon. The average Ar-blank value, measured in the clean extraction line, is on the order of $1 * 10^{-9}$ ccSTP⁴⁰Ar, the isotopic composition being that of air. However, the air-argon contribution rises during extraction of samples, due to air-argon content of sample and aluminium foil into which it is packed as well as differing air-argon release of the extraction line. A measured ⁴⁰Ar value for the foil is $1.7 * 10^{-8}$ ccSTP. As young amphiboles are poor in radiogenic Ar, differing contributions of air-Ar from the sample or extraction system are the main cause for scattering

Ar-errors. Ar-standards were measured during every set of runs. ⁴⁰Ar* concentrations in biotite LP-6 are 4186, 4214, and $4225 ± 46 * 10^{-8}$ ccSTP⁴⁰Ar*/g; 4 measurements on hornblende MMhb-1 yielded 3598, 3603, 3604, and $3617 ± 38 * 10^{-8}$ ccSTP⁴⁰Ar*/g. Potassium of MMhb-1 has been determined twice by isotope dilution, resulting in 1.541 and $1.552 ± 0.009$ weight %K.

Age results as calculated with the decay constants compiled by Steiger and Jaeger (1977) are given in Table 1. Errors are 2-sigma errors.

³⁹Ar-⁴⁰Ar data were obtained in Pisa on a MAT 240 spectrometer, which has the same tube geometry and an older prototype Baur-Signer source, GS 75. This machine is also used for ³⁸Ar spiked K-Ar, so that memory prevented ³⁸Ar measurement in Ar-Ar runs. Samples were irradiated in the Triga reactor in Pavia, using the age monitor B4M. The results are tabulated in Table 2 after machine background and mass discrimination corrections, but before Ca interference subtraction; errors are 1-sigma errors. Figure 5a-f plots ages from Table 2 with 2-sigma errors. Ages include Ca-correction. The errors on step ages only reflect within-step statistics; they do not include Ni-monitor counting errors (around 1%) and inter-irradiation bias (another 1%), so as not to obscure the significance of step age differences. Inter-sample comparison, however, requires compounding either Ni or (Ni + J) errors.

Table 2. Stepheating data. ^{40}Ar concentrations are in units of 10^{-7} ml/g, all other isotopes in units of 10^{-10} ml/g. For each sample, the line "Totals" shows the "radiogenic" ^{40}Ar (i.e. the sum of $^{40}\text{Ar}_{\text{tot}}$ minus 295.5 times the sum of ^{36}Ar) and the K concentration calculated from the sum of ^{39}Ar divided by the known production rate. These values can be compared with those, obtained independently, given in Table 1. For example LH 1, two totals were calculated: *A* including all steps, *B* excluding the lowest one (because it might represent cracking of a K-free fluid inclusion)

$T(^{\circ}\text{C})$	$^{40}\text{Ar}_{\text{tot}}$	$^{39}\text{Ar}_{\text{tot}}$	^{37}Ar	^{36}Ar	t (Ma)
Ze 4 P, 0.1038 g, $J=5.95 \text{ E-4}$					
700	2.227 ± 5	1.79 ± 3	64.9 ± 3	7.028 ± 37	93.0 ± 6.5
900	0.660 ± 5	2.79 ± 2	23.8 ± 2	1.862 ± 14	42.8 ± 1.7
1000	0.786 ± 12	20.17 ± 0.13	326.8 ± 2.0	1.489 ± 16	19.9 ± 0.4
1100	1.240 ± 5	48.37 ± 0.9	888.0 ± 2.7	1.420 ± 15	19.9 ± 0.1
1200	0.823 ± 5	24.97 ± 6	454.1 ± 2.4	1.315 ± 14	20.4 ± 0.2
1300	0.375 ± 1	1.63 ± 3	25.8 ± 0.1	1.122 ± 11	30.0 ± 2.2
1400	1.523 ± 4	0.27 ± 5	5.4 ± 0.5	5.061 ± 28	109.9 ± 37.9
Total:	$(^{40}\text{Ar}_{\text{rad}}=2.05)$ (K=0.237%)				22.3

Ze 4 L, 0.0909 g, $J=5.95 \text{ E-4}$					
700	1.963 ± 13	2.23 ± 8	65.0 ± 0.7	6.168 ± 29	70.1 ± 4.7
830	0.703 ± 7	2.60 ± 4	21.8 ± 4	1.905 ± 13	58.0 ± 1.9
940	0.583 ± 28	14.01 ± 0.31	185.4 ± 5.2	1.260 ± 33	17.4 ± 1.2
1000	0.836 ± 7	29.65 ± 9	451.5 ± 1.9	0.965 ± 17	21.3 ± 0.2
1050	0.428 ± 9	11.25 ± 0.10	163.6 ± 0.9	0.752 ± 10	21.0 ± 0.5
1140	0.945 ± 8	29.54 ± 0.11	450.7 ± 3.2	1.315 ± 38	21.6 ± 0.4
1200	0.693 ± 9	19.61 ± 8	288.2 ± 1.8	1.069 ± 16	22.0 ± 0.4
1270	0.366 ± 8	2.20 ± 0.11	34.0 ± 0.9	1.042 ± 14	29.7 ± 2.6
1350	0.405 ± 4	0.41 ± 6	6.0 ± 0.4	1.296 ± 13	59.6 ± 13.3
Total:	$(^{40}\text{Ar}_{\text{rad}}=2.39)$ (K=0.265%)				23.3

Ze 19 Core, 0.1018 g, $J=1.895 \text{ E-4}$					
700	0.861 ± 17	0.41 ± 1	2.85 ± 0.14	1.723 ± 32	272.3 ± 11.4
800	1.210 ± 4	0.47 ± 1	4.71 ± 0.11	2.436 ± 24	327.2 ± 9.9
900	0.534 ± 1	0.81 ± 1	3.25 ± 7	1.232 ± 14	70.5 ± 1.7
1000	0.530 ± 4	1.94 ± 4	16.41 ± 0.25	1.143 ± 32	34.0 ± 1.4

Table 2 (continued)

$T(^{\circ}\text{C})$	$^{40}\text{Ar}_{\text{tot}}$	$^{39}\text{Ar}_{\text{tot}}$	^{37}Ar	^{36}Ar	t (Ma)
1050	1.156 ± 6	8.75 ± 4	101.22 ± 0.49	1.522 ± 17	27.8 ± 0.3
1100	0.940 ± 7	6.38 ± 1	74.29 ± 0.36	1.386 ± 14	28.6 ± 0.3
1150	0.557 ± 4	2.89 ± 2	34.74 ± 0.21	1.030 ± 15	30.1 ± 0.6
1200	1.688 ± 4	9.84 ± 5	118.61 ± 0.46	2.867 ± 29	29.4 ± 0.3
1400	3.054 ± 5	5.47 ± 2	66.83 ± 0.26	8.536 ± 45	33.3 ± 0.8
Total:	$(^{40}\text{Ar}_{\text{rad}}=4.06)$ (K=0.279%)				37.1

Ze 19 Rim, 0.0945 g, $J=1.895 \text{ E-4}$					
700	1.050 ± 33	1.90 ± 0.12	4.6 ± 0.2	2.40 ± 2	60.4 ± 4.5
800	1.077 ± 54	0.74 ± 5	3.6 ± 0.5	2.44 ± 6	159.0 ± 11.4
900	0.425 ± 5	1.36 ± 2	3.9 ± 0.1	0.97 ± 2	34.8 ± 2.0
1000	0.526 ± 5	3.37 ± 6	28.1 ± 0.4	0.97 ± 4	24.2 ± 1.1
1050	1.043 ± 6	10.12 ± 8	116.4 ± 0.6	1.10 ± 2	24.5 ± 0.3
1100	0.609 ± 7	4.52 ± 6	49.4 ± 0.4	0.96 ± 2	24.8 ± 0.6
1150	0.806 ± 6	6.63 ± 4	74.4 ± 0.3	1.27 ± 2	22.6 ± 0.4
1200	0.634 ± 1	3.85 ± 2	41.4 ± 0.3	1.29 ± 2	22.8 ± 0.7
1400	1.196 ± 5	5.67 ± 3	56.9 ± 0.3	2.86 ± 4	21.5 ± 0.6
Total:	$(^{40}\text{Ar}_{\text{rad}}=3.15)$ (K=0.287%)				28.6

Ze 20, 0.0320 g, $J=7.94 \text{ E-4}$					
650	2.574 ± 8	6.10 ± 5	9.4 ± 0.1	8.37 ± 7	23.8 ± 4.7
750	1.222 ± 12	9.41 ± 6	5.8 ± 0.1	3.93 ± 6	9.3 ± 2.8
850	0.872 ± 9	9.16 ± 3	11.9 ± 0.1	2.72 ± 3	10.8 ± 1.4
950	1.701 ± 1	42.11 ± 0.12	280.9 ± 1.2	4.25 ± 5	15.9 ± 0.5
1000	1.119 ± 9	22.44 ± 6	202.8 ± 0.9	3.01 ± 4	15.8 ± 0.7
1100	4.152 ± 19	131.26 ± 0.25	1394.5 ± 4.3	8.52 ± 6	19.1 ± 0.2
1250	1.781 ± 10	30.04 ± 0.12	315.7 ± 1.2	4.66 ± 4	20.4 ± 0.5
Total:	$(^{40}\text{Ar}_{\text{rad}}=3.121)$ (K=0.45%)				17.8

PJ 3, 0.1119 g, $J=1.89 \text{ E-4}$					
680°	0.999 ± 1	1.01 ± 1	44.3 ± 4.4	3.291 ± 35	10.7 ± 3.6

Table 2 (continued)

$T(^{\circ}\text{C})$	$^{40}\text{Ar}_{\text{tot}}$	$^{39}\text{Ar}_{\text{tot}}$	^{37}Ar	^{36}Ar	t (Ma)
PJ 3, 0.1119 g, $J=1.89 \text{ E-4}$					
900°	0.896 ± 1	1.56 ± 2	31.8 ± 3.2	2.795 ± 24	16.0 ± 1.6
1000°	0.706 ± 1	4.95 ± 1	13.1 ± 5.9	1.620 ± 17	16.1 ± 0.4
1100°	1.665 ± 2	16.03 ± 4	232.0 ± 6.9	2.720 ± 20	18.8 ± 0.1
1150°	1.334 ± 2	9.65 ± 3	143.0 ± 5.7	2.786 ± 24	18.5 ± 0.3
1250°	0.907 ± 1	1.01 ± 1	15.9 ± 2.4	2.905 ± 22	17.0 ± 2.2
Total:	$(^{40}\text{Ar}_{\text{rad}}=1.79) \text{ (K}=0.259\%)$				18.0
PJ 6, 0.0826 g, $J=4.7 \text{ E-4}$					
700	7.12 ± 7	6.92 ± 0.21	89.6 ± 1.1	21.09 ± 0.11	107.6 ± 6.1
800	2.92 ± 4	2.96 ± 0.11	30.3 ± 0.7	8.32 ± 5	130.1 ± 6.4
1000	2.77 ± 5	15.63 ± 0.16	235.7 ± 3.7	7.54 ± 4	30.7 ± 0.9
1050	2.77 ± 4	14.07 ± 0.14	238.6 ± 3.7	7.74 ± 4	30.2 ± 0.9
1100	3.53 ± 4	19.72 ± 0.12	338.5 ± 1.7	10.15 ± 6	24.1 ± 0.8
1150	4.22 ± 4	13.01 ± 0.13	226.3 ± 2.3	12.90 ± 0.14	27.8 ± 2.6
1200	5.89 ± 3	9.38 ± 0.11	163.6 ± 1.1	18.93 ± 9	27.6 ± 2.3
1500	27.69 ± 3	5.97 ± 4	97.6 ± 0.8	92.32 ± 0.38	58.3 ± 15.5
Total:	$(^{40}\text{Ar}_{\text{rad}}=4.13) \text{ (K}=0.266\%)$				39.5
LH 1, 0.1037 g, $J=2.6 \text{ E-4}$					
650	97.83 ± 0.14	0	0	316.42 ± 1.24	–
900	16.07 ± 1	4.57 ± 3	29.2 ± 0.2	50.86 ± 0.19	104.1 ± 5.4
1000	14.96 ± 1	12.65 ± 3	124.3 ± 0.5	47.01 ± 0.18	39.7 ± 1.9
1050	3.309 ± 3	8.90 ± 2	85.1 ± 0.4	9.52 ± 7	26.5 ± 1.0
1100	2.922 ± 4	8.06 ± 5	78.9 ± 0.3	8.47 ± 4	24.7 ± 0.8
1150	3.491 ± 2	29.05 ± 7	309.9 ± 0.9	5.65 ± 4	29.8 ± 0.2
1200	0.901 ± 1	4.47 ± 1	45.8 ± 0.2	2.15 ± 3	28.2 ± 1.0
1400	2.415 ± 2	2.22 ± 1	19.3 ± 0.1	7.76 ± 5	26.1 ± 3.0
Total A:	$(^{40}\text{Ar}_{\text{rad}}=9.61) \text{ (K}=0.384\%)$				63.1
Total B:	$(^{40}\text{Ar}_{\text{rad}}=4.28)$				35.1

Table 2 (continued)

$T(^{\circ}\text{C})$	$^{40}\text{Ar}_{\text{tot}}$	$^{39}\text{Ar}_{\text{tot}}$	^{37}Ar	^{36}Ar	t (Ma)
LH 3, 0.0920 g, $J=2.6 \text{ E-4}$					
750	0.936 ± 1	1.465 ± 22	not measured	2.597 ± 37	53.3 ± 3.5
900	0.2625 ± 4	1.859 ± 11	not measured	0.614 ± 29	20.3 ± 2.2
950	0.1609 ± 2	1.679 ± 77	not measured	0.366 ± 29	14.5 ± 2.5
1000	0.1725 ± 3	1.961 ± 11	not measured	0.343 ± 29	16.9 ± 2.1
1030	0.3735 ± 3	4.632 ± 23	not measured	0.576 ± 30	20.5 ± 0.9
1060	0.7076 ± 7	10.005 ± 51	not measured	0.795 ± 29	22.5 ± 0.4
1100	0.7963 ± 5	12.384 ± 25	not measured	0.786 ± 30	21.8 ± 0.3
1200	2.274 ± 1	29.600 ± 52	not measured	2.539 ± 36	24.6 ± 0.2
1400	3.010 ± 2	4.293 ± 35	not measured	9.428 ± 58	24.7 ± 1.8
Total:	$(^{40}\text{Ar}_{\text{rad}}=3.41) \text{ (K}=0.373\%)$				23.5
LH 6, 0.1122 g, $J=2.6 \text{ E4}$					
700°	1.399 ± 1	1.31 ± 3	10.1 ± 0.1	3.17 ± 5	159.6 ± 5.9
900°	1.711 ± 1	14.29 ± 4	163.3 ± 0.5	2.94 ± 5	28.1 ± 0.5
1000°	2.640 ± 3	30.15 ± 7	336.1 ± 0.9	3.84 ± 5	23.9 ± 0.3
1030°	1.783 ± 2	6.86 ± 1	79.7 ± 0.3	4.62 ± 6	29.0 ± 1.1
1060°	1.596 ± 2	4.23 ± 1	48.5 ± 0.2	4.45 ± 6	31.5 ± 1.9
1100°	2.363 ± 2	2.57 ± 1	28.0 ± 0.1	7.10 ± 6	48.4 ± 3.1
1130°	4.192 ± 4	2.91 ± 3	33.5 ± 0.2	13.02 ± 8	55.7 ± 3.8
1400°	5.202 ± 5	1.38 ± 3	14.9 ± 0.1	16.82 ± 9	78.2 ± 8.8
Total:	$(^{40}\text{Ar}_{\text{rad}}=4.41) \text{ (K}=0.339\%)$				33.2

K-Ar dating of amphiboles

Results of age determinations are given in Table 1. Inconsistencies between amphibole ages and the microfabric and mineralogical observations are evident. The scatter of amphibole ages at Zemmgrund deserves some detailed discussion, emphasizing the problem of excess Ar.

Essentially two hornblende age groups are observed at Zemmgrund with apparent ages of 19 and 24 Ma. The high ages for both core and rim of hornblende Ze 19 will be discussed later. The cummingtonites yield 120 Ma, although errors are large for this mineral because the $^{40}\text{Ar}^*$ concentration is low. As discussed by Blanckenburg and Morteani (1988) *only one* generation and growth period has been re-

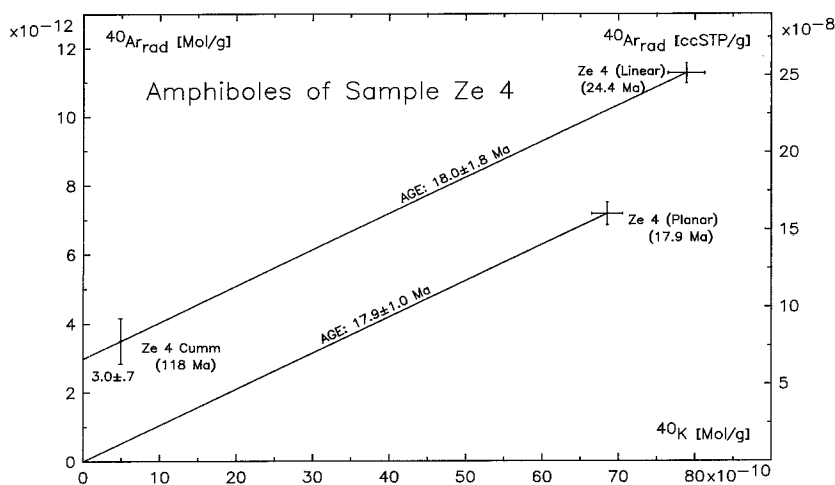


Fig. 3. $^{40}\text{Ar}_{\text{rad}}$ versus ^{40}K isochron plot for sample Ze 4. Hornblende Ze 4P was arbitrarily assumed to contain no excess and defines the lower "isochron". The upper "isochron" combines a cummingtonite (whose model age of 120 Ma is surely due to excess) with hornblende Ze 4L (24.4 Ma). The intercept value corresponds to $6.7 \pm 1.6 \times 10^{-8}$ ccSTP/g

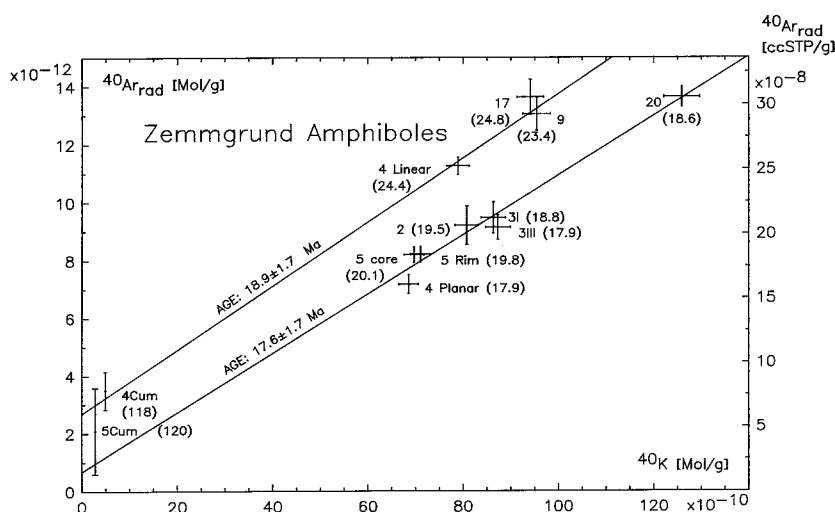


Fig. 4. Same diagram as Fig. 3, showing all amphiboles from Zemmgrund except Ze 19. The upper reference line is defined by excess-Ar bearing amphiboles, the lower by presumably excess-free minerals. (Model ages are given in parentheses. This diagram serves for illustrational purposes only.)

cognized for all amphiboles and no major chemical differences are seen between green hornblendes of different samples. Consequently all amphibole ages should fall into a narrow range, independent of their interpretation as growth or cooling ages since they originate from a restricted area. As this is not the case, evidently there is excess Ar present in at least some of the samples. In particular the cummingtonite ages of 120 Ma are geologically meaningless and reflect excess Ar.

The complex pattern can be resolved in the key sample Ze 4, from which planar hornblende (17.9 Ma), a linear hornblende (24.4 Ma) and a cummingtonite (118 Ma) coexisting with both hornblendes yield three different apparent ages. A rough calculation shows that by subtraction of equal amounts of excess-Ar (6.6×10^{-8} ccSTP/g $^{40}\text{Ar}^*$) from both cummingtonite and linear hornblende we obtain an age of ~ 18 Ma for all three amphiboles. This approach seems feasible because cummingtonite as a member of the amphibole group may, but not must, incorporate excess Ar in similar sites and quantity as hornblende. This situation is illustrated by the isochron in Fig. 3. Note that it is impossible to fit all three amphiboles to a single isochron! If the intercept value of Fig. 3 is used to correct the other ages of the 24 Ma group (Table 1), the individual age of Ze 9 changes from 23.4 Ma to 18.0 ± 1.9 Ma and for Ze 17 from 24.8 to 19.3 ± 2.0 Ma, the larger uncertainty being

due to the high excess-Ar error. The plausibility of this intercept value is demonstrated in Fig. 4. The isochrons fitted through the data field of the 24 Ma hornblendes and cummingtonites by the least-square method (York 1969) yields a slope corresponding to 18.9 Ma and that through the field of the younger samples a slope of 17.6 Ma. The two isochrons coincide within limits of error.

Of course, K-Ar isochrons are not claimed to give accurate solutions for every confusing K-Ar age pattern affected by excess Ar. Roddick et al. (1980, p.203) demonstrate restrictions of K-Ar isochrons because "trapped" $^{40}\text{Ar}/^{36}\text{Ar}$ may have variable but unknown isotopic compositions. Villa (1983) points to the mobility of Ar, which may lead to an illegitimate use of the K/Ar isochron. Thus, the systematics of the data array in Fig. 4 may well be an effect of pure coincidence. The mobility of excess ^{40}Ar is indicated by the scatter of the data points with respect to the best fit lines; especially samples Ze 2, Ze 5 core and rim seem to indicate higher excess ^{40}Ar -concentration in comparison to the other samples. Their ages of 19–20 Ma might therefore still be too high. However, several conclusions can be drawn from the K-Ar analysis: (1) Conventional K-Ar techniques may give semiquantitative indication of the excess-Ar concentration if coexisting amphiboles of the same generation but with considerably different K-concentrations are dated. (2) The excess-Ar concentration may vary

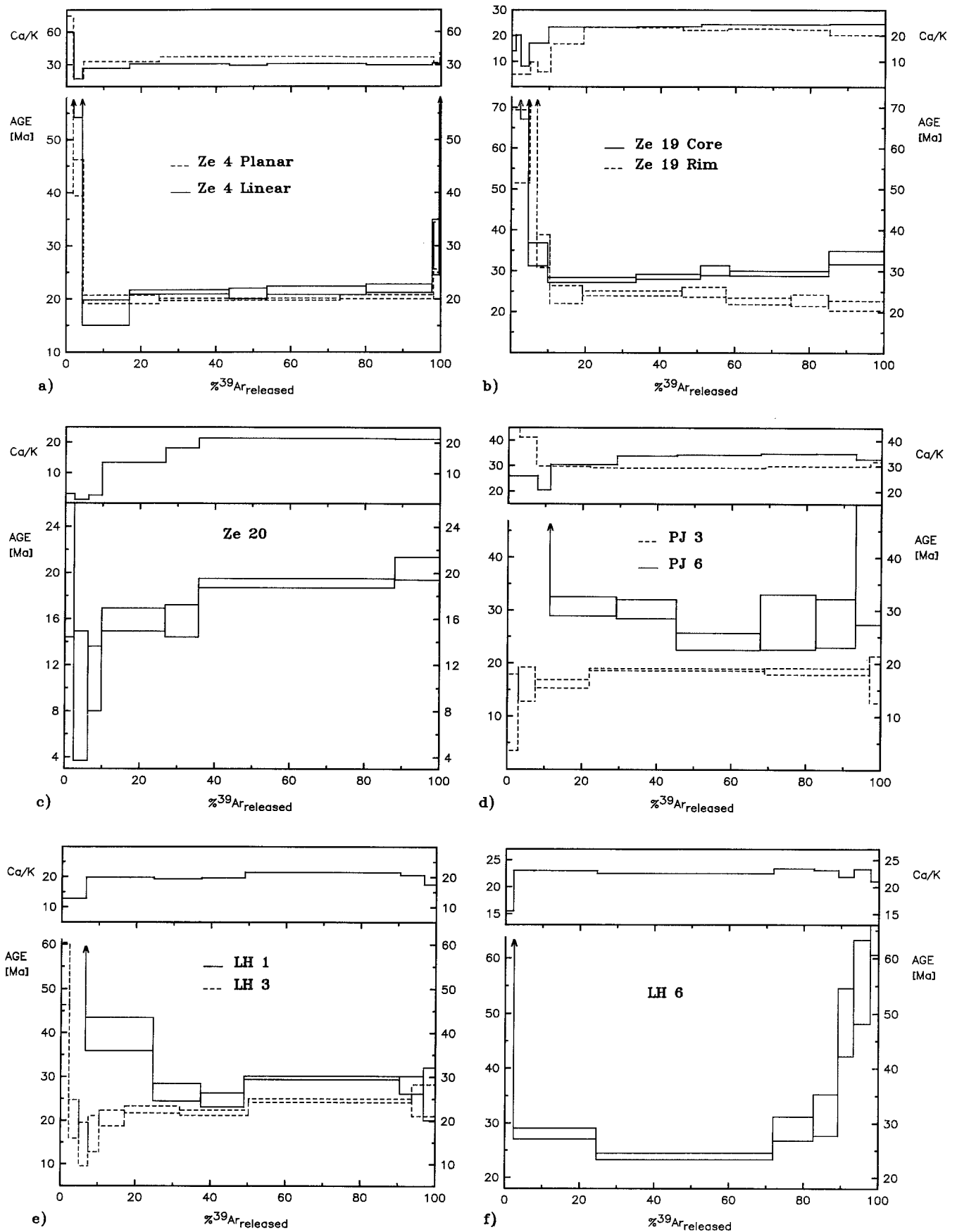


Fig. 5a-f. ^{39}Ar - ^{40}Ar release- and Ca/K-spectra of hornblendes

within centimeters of a hand specimen and – more seriously – is distributed irregularly even between carefully split sample aliquots. (3) The youngest observed ages approach the probable “undisturbed” K-Ar age of the sample group, which is 18–19 Ma in this case. (4) Dating of a *single* amphibole from one sampling locality may lead to erroneous model ages, as only the age scatter of a large number of samples may reveal excess-Ar.

Exceptionally high K-Ar ages of 33.9 and 28.9 Ma were measured for core and rim, respectively, of the coarse-grained, inclusion-poor hornblende Ze 19. The strongly poikiloblastic medium-grained hornblende Ze 5, in contrast, yielded ages of 20.1 Ma for the core and 19.8 Ma for the rim, which were used for calculation of the lower isochron of Fig. 4. The age difference between the two hornblendes, however, has no geological reason, as ^{39}Ar – ^{40}Ar spectra for Ze 19 core and rim reveal excess argon.

At Pfitscher Joch, 4 hornblendes have ages in the range of 16.8–18.5 Ma, the one 30.7 Ma outlier, PJ 6, is again a result of excess Ar, as shown by the Ar-Ar method.

K-Ar apparent ages of hornblendes at Landshuter Hütte are widely scattered between 24 and 37 Ma. Such an age jump could be indicative of transition from cooling to formation ages. However, plain evidence for excess Ar is already given by the inhomogeneity of the two splits of sample LH 1, which give different ages of 33.5–37.3 Ma, clearly outside analytical error. Ar-Ar analysis demonstrates that all three LH hornblendes contain excess Ar.

Geological reasons for the incorporation of excess Ar into amphiboles are discussed in the next section.

Hornblende ^{39}Ar – ^{40}Ar Ar ages

Ar-Ar spectra on 10 hornblende samples display a variety of shapes, sketched in Fig. 6. Types a and b define a high-temperature plateau and give meaningful age information; types c and d do not define a plateau and only point to an asymptotic age, which is no better defined than “less or equal to the youngest step”. The significance of the younger step ages in types a and b will be discussed below, comparing their numerical values with other chronometers. In most cases the integrated Ar-Ar ages agree with the K-Ar ages, except in three cases. Since sample inhomogeneity seems rather common, and samples were separated anew from different fractions of the original mineral concentrate, it is likely that these three age discrepancies are due to differences of 2–3 pico-liters excess Ar, e.g. one large fluid inclusion. If the cause of the discrepancy were some instrumental artefact, the integrated K value would be affected as well, but it always agrees with the isotope dilution data (Table 1).

Individual release spectra are shown in Fig. 5 a–f, together with the Ca/K spectrum. The two hornblendes of Ze 4, linear (L) and planar (P) (see above and Fig. 3) are shown in Fig. 5a. The presence of excess Ar in Ze 4L is confirmed. However, also Ze 4P gives a “type d” saddle spectrum, and its integrated age is 20% higher than the K/Ar age. In 4P, a quasi-plateau comprising 3 steps and 93% of the gas averages 20.0 Ma, with a nearly constant Ca/K of about 35. Interestingly, the better “plateau” is that of Ze 4L, where four steps with 83% of the gas average 21.5 Ma. It would be very tempting to ascribe the 4L plateau a chronological meaning, since it satisfies the usual

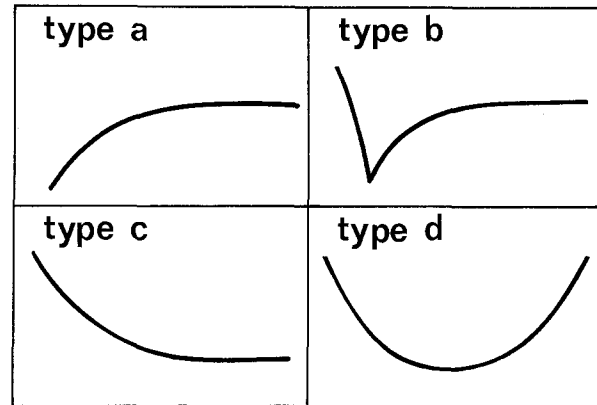


Fig. 6. Schematic diagrams showing different types of release spectra

criteria (4 or more consecutive steps containing over 10% gas each and no further than 2 sigma from the average). One argument against this “plateau age” is the petrographical observation of the simultaneous growth of 4P and 4L (Blanckenburg and Morteani 1988), implying that the above criteria are necessary, but not sufficient, conditions, and that one specimen can give two discordant plateaus, one of which has absolutely no chronological meaning. The second, antithetical, explanation is that *both* plateaus represent cooling ages: 4P and 4L would record closure temperatures (T_c) about 50° C apart. This hypothesis has one fundamental difficulty, that T_c is postulated to be different despite the chemical similarity of the two hornblendes, but it has the attractive feature of upholding one of the strongholds of Ar-Ar dating, the significance of plateaus.

In this light, most of the subsequent discussion on the chronological data from Fig. 5 is academic, since the two remaining plateaus also might be “false excess plateaus”. However, some other conclusions still can be drawn. Ze 20 (Fig. 5c) is a type b spectrum, with a two-step flat portion at 18 Ma. Ze 19 (Fig. 5b) shows that neither core nor rim K-Ar ages are crystallization or formation ages, since both contain a very large low-temperature excess. The rim (type c spectrum) tends towards 20 Ma. The core (type d) incorporated excess Ar more pervasively and its saddle allows no sensible age conclusion. Fluid inclusions alone would not release excess Ar over the whole temperature range, so part of it must be held in lattice portions. We note that the persistence of this large Ar excess (ca. 16×10^{-8} ml/g) can be reconciled with the model sketched below, i.e. large Ar overpressure during formation and deformation of hornblendes, by assuming that this particular sample had a higher retentivity than the rest of the Ze samples.

Spectra of PJ hornblendes are shown in Fig. 5 d. PJ 6 (type d) has a saddle minimum at 23.8 Ma (i.e. $t < 23.8$ Ma), and the real age would approach the three-step type a plateau of PJ 3 (Fig. 5d, 18 Ma). This latter age is very similar to that of Ze 20. Finally, LH hornblendes (Fig. 5e, f) display all varieties of excess Ar spectra: type b (LH 3), type c (LH 1), and type d (LH 6). “Ages” tend towards 20 Ma, but are obscured by larger concentrations of excess Ar than both Ze and PJ. The tectonic peculiarity of location LH, which is a small garbenschiefer lens in the Hercynian Zentralgneis, accounts very well for the excess Ar abundance (see also next section).

Discussion

Incorporation of excess argon into hornblende

In the previous section it was shown that the scatter in hornblende ages is mainly due to small but somewhat variable amounts of excess Argon and not to growth of more than one generation of hornblende. The degree of contamination by excess Ar is *high* in minerals surrounded by K-rich and thus ^{40}Ar -rich rocks e.g. Landshuter Huefte, where the garbenschists occur as small lenses in the Hercynian Zentralgneis, and PJ 6, which is located directly on the contact with the Zentralgneis. Under such conditions even biotite ages may be erroneous (Blanckenburg et al. 1988). In pure garbenschist horizons, ^{40}Ar is present during metamorphism due to continuous degassing of K-bearing minerals, mainly biotite, being held above their closure temperature. The structural development of the amphiboles (Blanckenburg and Morteani 1988) explains very well the release and irregular incorporation of excess Ar in variable amounts even on the scale of an individual sample. During the formation of s_2 cracks the rock was intensely deformed at rather high pressures. Such an event forms the pathways for a circulating fluid phase which acts as a sink for ^{40}Ar released from K-rich minerals. During the static recrystallization that followed the tectonism producing s_2 the excess Ar bearing fluid was trapped preferentially in the annealed cracks of the border zones of the amphiboles, most probably in fluid inclusions. Fluid inclusions are known to carry excess Ar (Rama et al. 1965). The tensional deformation s_3 was connected with uplift, decreasing pressures but still high temperatures. During this stage aliquots of the trapped excess Ar were released depending upon the degree of the tensional deformation of the individual rock samples. The scatter of the amount of excess ^{40}Ar is thus explained by the incorporation and partial loss of excess Ar during the different stages of deformation and tempering. A similar process was discussed by Stoeckhert et al. (1986) for kinked phengites from the western Alpine Sesia Zone. The absence of excess Ar from PJ and Ze biotites (Blanckenburg et al. 1988) could be due (1) to the fact that the Ar-loss phase lasted longer than for hornblende, (2) to the different deformational history, or (3) to the absence of fluid inclusions. The particular tectonic evolution explains the absence of real age differences between hornblendes of different fabric orientation. Such a correlation was observed by Steiger (1964) along the N margin of the Central Alps. In the present study the measured age differences between linear and planar hornblendes are probably the result of an irregular concentration of ^{40}Ar bearing fluid inclusions accidentally distributed in different amounts between sample splits.

Interpretation of Ar-Ar spectra in hornblende

In theory, type a spectra (Fig. 6) should represent the partially degassed lognormal spheres of Turner (1968); low ages must be explained in terms of Ar loss from the hornblende. Type b could either represent an Ar loss type (type a) with superimposed excess, or a recoil redistribution of ^{39}Ar , away from the very rim into an intermediate catcher area. Since recoil affects ^{37}Ar and ^{39}Ar in a very similar way, recoil-caused age dips should be accompanied by only slight variations in the Ca/K ratio as the recoiling atoms are superimposed on the indigenous atoms of the catcher area. If, on the contrary, the Ca/K ratios were strongly

variable, then this means that the inhomogeneities of the degassed sites predominate over the recoiled atoms, and that the plunge of type b spectra results from Ar loss from hornblende.

In these samples, as in most literature data, the Ca/K ratio is irregular in the first 20–30% of the ^{39}Ar release and then settles for a “plateau” comprising the remaining 70–80%. The constancy of the Ca/K ratio displayed by the higher temperature steps can be explained as follows. K and Ca occupy two different crystallographic sites (A and M⁴) with different ion binding energies; reactor-produced, neutral ^{39}Ar and ^{37}Ar only experience van der Waals forces, which are notoriously substantially weaker than ionic forces. On the other hand, the constancy of the Ca/K ratio indicates the same binding energy for ^{37}Ar (M4 site) and ^{39}Ar (A site) despite the differences in the surrounding ion fields; this means that Ar release from the crystal is not controlled by its parent’s crystallographic site. The fact that the retentivities and thus activation energies for neutral Ar diffusion are comparable to that for charged ions means that both diffuse via the same mechanism; not interstitial migration of neutral atoms, but rather defect migration. Physical mechanisms for diffusion are reviewed by Manning (1974); the equations describing them require knowledge of many parameters, so that no application to minerals has ever been attempted. Speculations on this point will be presented elsewhere (Villa in prep.). A logical consequence is that the irregularities in the first quarter of the release do not derive from fluctuations in the activation energy E but rather in the diffusion length. In other words, the low-T part of the release is dominated by domains whose diffusivity D/a^2 is large because a is very small, i.e. probably very fine exsolutions of Ca-rich and Ca-poor phases, so that the overall Ca/K is irregular. The greater part of K is usually contained in what appears to be an exsolution-free crystal structure with constant Ca/K.

The curious thing about this dichotomy is the behaviour with respect to diffusive Ar loss. In the only published instance of stepwise heating of a hornblende preheated at hydrothermal conditions (Harrison 1981), close scrutiny of the data reveals that:

- ^{40}Ar was lost in major amounts only from sites with $\text{Ca/K} < 10$
- Little or no ^{40}Ar was lost in the temperature steps with $\text{Ca/K} > 25$.

The preliminary conclusion from this very limited data set of one sample is that microstructurally peculiar domains were almost totally reset during hydrothermal treatment, but the “healthy” part of the crystal was not. The “closure” behavior, at least for hornblende 77–600 (Harrison 1981) thus appears to reflect the relative proportion of microstructural complexities rather than to follow isotropic sphere models. The calculated “activation energy” for 77–600 might therefore also be a spurious mixing effect as was that of the North Walpole hornblende (Harrison and Fitz Gerald 1986). A correlation between non-equilibrium Ca/K region and rejuvenated ages is seen in the type a and b spectra of the present work. Sample PJ 3 (Fig. 5d) shows $\text{Ca/K} > 90$ for $t < 11$ Ma and $\text{Ca/K} = 29\text{--}30$ for $t = 17\text{--}18$ Ma. Ze 20 has almost constant Ca/K ratios in the first three steps, at 2.3 ± 0.9 . Lumped together, their averaged age is 13 Ma, significantly lower than the plateau around 19 Ma. Unfortunately, no ^{37}Ar data were obtained for LH 3. Comparing the Ar loss spectra with Turner’s

(1968) lognormal sphere model, one would infer that a recent disturbance, which occurred later than 10 Ma ago, degassed the hornblendes and induced Ar losses of 4% (PJ 3), and 7% (Ze 20). However, the geological implications for such a young, thermal event are untenable. Argon loss from a homogeneous tschermakitic hornblende would require high temperatures (see Table 1 of Blanckenburg et al. 1988) but apatite FT ages indicate temperatures in the range of 100° C for this time. A short-lived thermotectonic event (shearing) is excluded by petrography. The explanation is that the anomalously low age steps correspond to fine-grained exsolved Ca-poor (Ze 20) or Ca-rich (PJ 3) phases which are easier to degas than the bulk of the sample. Note that the trends in the Ca/K ratios have absolutely no geometrical meaning, since the original rims and cores of the crystals were mixed together by the crushing; above all, both rim and core of Ze 19 show a low-temperature drop in the Ca/K ratio, which therefore must reflect microstructurally controlled retentivity changes. Changes in retentivity caused by microstructural exsolution of chemically distinct phases were demonstrated by Harrison and Fitz Gerald (1986) and Onstott and Peacock (1987). The existence of patches of irregular Ar retentivity in single crystals was discovered by laser microprobe (Kelley and Turner 1987). Although electron microprobe data on the examined specimens were not given, it is straightforward to assume that the fact that metamorphosed mineral grains display undegassed patches tightly adjacent to rejuvenated patches (at a resolution of ca. 0.1 mm) can only mean that metamorphosed minerals are not uniform, isotropic spheres but patchy aggregates of leaky and retentive allotropes. It is extremely likely that what is seen as “patch” with the resolution of the laser microprobe is actually a region of finer exsolution lamellae that could be made visible only with TEM resolution.

Compositional effects

The narrow range of undisturbed K-Ar cooling ages and plateau ages from type a and type b for hornblendes from all three locations indicate similar closure temperatures (T_c) for all of them. Thus, no very large compositional effects on the closure temperature are seen. Blanckenburg and Morteani (1988) have shown that the compositional range of tschermakites is narrow, with Mg/Fe being the only really variable component. At the level of 1 Ma either Mg/Fe plays no role or another unknown contrary parameter is active. No conclusions, however, can be drawn with respect to the influence of the other components because of their low variability in the hornblendes of this study. Therefore, it cannot be excluded that hornblendes of compositions significantly different from the studied tschermakites display completely different closure temperatures. Influence of other parameters beside the Mg/Fe ratio is demonstrated by the preferred resetting of cummingtonite as observed by Harrison and Fitz Gerald (1986). This effect is not confirmable by the data presented here as the cummingtonite ages are severely disturbed by excess Ar.

Reasons for variable retentivity

The key question at this stage of the discussion must be: What is, exactly, a usable definition of T_c ? We shall leave aside the fundamental question if laboratory loss involve one and the same mechanism, and if approximating either one by volume diffusion of neutral atoms really is accurate.

In this approximation, for a given sample, a series of laboratory experiments can determine the activation energy (E) and diffusion coefficient (D_0) and thus T_c for that particular sample. In order to be geologically useful, however, T_c should be determined on selected standard minerals and be valid for any unknown sample. That this is not the case is recognized from Table 1 (Blanckenburg et al. 1988), where, for example, “biotite T_c ” is seen to be a rather variable constant. The worst surprises come from more detailed studies, where textural effects on all scales (sub-micron to millimeter) and multi-parameter cation substitutions make the retention behavior extremely variable. So, for instance, it may be futile to speculate whether or not Fe/Mg has an influence on the T_c of minerals if other equally important crystal chemical parameters, such as simple and coupled substitutions, Fe^{2+}/Fe^{3+} , A-site occupancy, dioctahedral-trioctahedral exchange etc., and lattice constants are neglected. It is, in principle, possible to calculate diffusion rates of neutral Ar atoms from lattice ionic potentials and electronic wave functions for samples whose intimate structure has been characterized by TEM and Moessbauer-spectroscopy; but then we postulate that only temperature had an influence, and that the mineral underwent absolutely no reaction with the metamorphic fluid, and does not have the patchy structure seen in real life.

For the following reason the results of this study still support application of some closure temperature to reconstruct PTt-paths: (1) Several of the above problems may be minimized by the good control over the mineralogical parameters of the minerals dated in this study; (2) The scale of this project, 32 samples in a restricted area, ensures good statistics, so that *on average* most of these hornblendes, which are chemically very similar (Blanckenburg and Morteani 1988) will behave similarly with respect to a metamorphic event which affected the 12 by 3 km wide LSH with reasonably similar P , T , and P_{H_2O} . Indeed, the isotopic ages are fairly constant and the ages can find a consistent explanation for the small extent of the region studied. In the present case of a restricted area, limited use of the T_c concept may be acceptable.

Conclusions

K-Ar and ^{39}Ar - ^{40}Ar data of the studied amphiboles point to two major interferences occurring when studying young, K-poor amphiboles: Excess-Ar and variable retentivity.

Excess-Ar is incorporated differentially into amphiboles (i) in lattice sites during crystallization, (ii) in fluid inclusions which are produced mainly by fracturing and subsequent annealing of amphiboles during the temperature maximum. These excess Ar amounts are distributed irregularly even between two splits of the same sample and are substantial in 12 out of 22 amphiboles. This high fraction of excess Ar bearing amphiboles suggest that with a high probability K-Ar dating of single hornblende samples will yield erroneous results. Excess-Ar is detected by (1) K-Ar measurements in the nearly K-free cummingtonites, (2) the scatter of K-Ar ages of larger number of samples from a single location, or (3) by ^{39}Ar - ^{40}Ar release spectra of type *c* and *d*.

These spectra exhibit different shapes. In three cases, where sufficiently small amounts of excess Ar were present, geologically meaningful ages of 18–20 Ma were obtained from type *a* and *b* spectra. In one case a plateau of a higher age was obtained from a type *d* spectrum but comparison

with K-Ar ages, the uniform metamorphic history, and the overall narrow compositional range of hornblendes suggest that this class of plateaus has no geological meaning, i.e. they are “false excess plateaus”, although a chronological interpretation involving a higher T_c cannot be completely ruled out.

After establishing the presence of excess Ar, “corrected” K/Ar ages can be calculated to be around 18 ± 0.8 Ma. Asymptotic low temperature steps with ages < 10 Ma and disturbed Ca/K spectra of type *a* and *b* spectra give hints for submicroscopic exsolution domains in amphibole with a considerably lower Ar activation energy and a smaller diffusion length.

This observation and the difference of the studied cooling age sequence (Blanckenburg et al. 1988) from sequences in other terranes leads to the conclusion that “closure temperatures” appear to be regionally variable, rather than fixed. Firstly, a number of parameters other than Mg/Fe²⁺ (e.g. single and coupled substitutions, A-site occupancy, dioctahedral/trioctahedral exchange, presence and properties of a fluid phase) influence Ar retention, but up to now their systematics have been totally neglected. Secondly, low temperature steps with ages < 10 Ma and variable Ca/K give evidence for submicroscopic exsolution domains with different mineralogies and different Ar retentivity in metamorphic hornblendes, which are thus not at all the isotropic media of the closure temperature model.

Acknowledgements. At ETH Zurich, Mrs. Irene Ivanov is thanked for help in the isotope dilution analyses of Ze-samples and Heiri Baur for introduction into Ar-measurements. O. Giuliani helped maintain the Pisa laboratory. We acknowledge discussions and critical reviews by Jane Selverstone, Muharrem Satir and Felix Oberli and an anonymous reviewer. The first author acknowledges financial support by ETH grant 0.330.085.51/5.

References

- Berry RF, Mc Dougall I (1986) Interpretation of ⁴⁰Ar/³⁹Ar and K-Ar dating evidence from the Ailu Formation, East Timor, Indonesia. *Chem Geol* 59:43–58
- Besang Cl, Harre W, Karl F, Kreuzer H, Lenz H, Mueller P, Wendt J (1968) Radiometrische Altersbestimmungen (Rb/Sr und K-Ar) an Gesteinen des Venediger-Gebietes (Hohe Tauern, Österreich). *Geol Jb* 86:835–844
- Blanckenburg F v, Morteani G (1988) Crystallization and deformation of amphiboles and cumingtonite forming reactions in the garbenschists of the Western Tauern Window (Eastern Alps). *Lithos*, submitted for publication
- Blanckenburg F v, Villa I, Baur H, Morteani G, Steiger RH (1988) Time calibration of a PT-path in the Western Tauern Window, Eastern Alps: The problem of closure temperatures. *Contrib Mineral Petrol*, submitted for publication
- Cliff RA, Norris RJ, Oxburgh ER, Wright RC (1971) Structural, metamorphic and geochronological studies in the Reisseck and southern Ankogel groups, Eastern Alps. *Jahrb Geol Bundesanstalt Austria* 114:121–272
- Cliff RA, Droop GTR, Rex DC (1985) Alpine metamorphism in the south-east Tauern Window, Austria: 2. Rates of heating, cooling and uplift. *J Metamorphic Geol* 3:403–415
- Dalrymple GB, Lanphere MA (1969) Potassium-Argon Dating: Principles, Techniques and Applications to Geochronology. Freeman 258pp
- Deutsch A, Steiger RH (1985) Hornblende K-Ar ages and the climax of tertiary metamorphism in the Lepontine Alps (south-central Switzerland): An old problem reassessed. *Earth Planet Sci Lett* 72:175–189
- Deutsch A, Steiger RH (1986) A reassessment appraised: comment on “Hornblende K-Ar ages and the climax of tertiary metamorphism in the Lepontine Alps (south-central Switzerland): an old problem reassessed” – reply to Peter K Zeitler and Jan R Wijbrans. *Earth Planet Sci Lett* 76:393–395
- Hanson GN, Gast PW (1967) Kinetic studies in contact metamorphic zones. *Geochim Cosmochim Acta* 31:1119–1153
- Harrison TM (1981) Diffusion of ⁴⁰Ar in hornblende. *Contrib Mineral Petrol* 78:324–331
- Harrison TM, Mc Dougall I (1980) Investigations of an intrusive contact, northwest Nelson, New Zealand-II. Diffusion of radiogenic and excess ⁴⁰Ar in hornblende revealed by ⁴⁰Ar/³⁹Ar age spectrum analysis. *Geochim Cosmochim Acta* 44:2005–2020
- Harrison TM, Mc Dougall I (1981) Excess ⁴⁰Ar in metamorphic rocks from Broken Hill, New south Wales: Implications for ⁴⁰Ar/³⁹Ar age spectra and the thermal history of the region. *Earth Planet Sci Lett* 55:123–149
- Harrison TM, Fitz Gerald JD (1986) Exsolution in hornblende and its consequences for ⁴⁰Ar/³⁹Ar age spectra and closure temperature. *Geochim Cosmochim Acta* 50:247–253
- Kelley S, Turner G (1987) Laser probe ⁴⁰Ar-³⁹Ar age profiles across single hornblende grains from the Giants Range granite, Northern Minnesota, USA (abstract). *Terra Cognita* 7:285
- Lammerer B (1986) Das Autochthon im westlichen Tauernfenster. *Jahrb Geol Bundesanstalt Austria* 129:51–67
- Manning JR (1974) Diffusion kinetics and mechanisms in simple crystals. In: Hoffmann et al. (eds) *Geochemical transport and kinetics*, Carnegie Institution of Washington:3–13
- Morteani G (1974) Petrology of the Tauern Window, Austrian Alps. *Fortschr Miner* 52/1:195–220
- O’Nions RK, Smith DGW, Baadsgaard H, Morton RD (1968) Influence of chemical composition on argon retentivity in metamorphic calcic amphiboles from south Norway. *Earth Planet Sci Lett* 5:339–345
- Onstott TC, Peacock MW (1987) Argon retentivity of hornblendes: A field experiment in a slowly cooled metamorphic terrane. *Geochim Cosmochim Acta* 51:2891–2903
- Rama SNI, Hart SR, Roedder EV (1965) Excess radiogenic argon in fluid inclusions. *J Geoph Research* 70:508–511
- Raith M, Raase P, Kreuzer H, Mueller P (1978) The age of the Alpidic metamorphism in the western Tauern Window, Austrian Alps, according to radiometric dating. In: Closs H, Roeder D, Schmidt K (eds) *Alps, Apennines, Hellenides Inter-Union Comm on Geodynamics Sci Rep* 38:140–148
- Roddick JC, Cliff RA, Rex DC (1980) The evolution of excess argon in Alpine biotites – a ⁴⁰Ar-³⁹Ar analysis. *Earth Planet Sci Lett* 48:185–208
- Selverstone J, Spear FS, Franz G, Morteani G (1984) High-pressure metamorphism in the SW Tauern Window, Austria: P-T paths from hornblende-kyanite-staurolite schists. *J Petrol* 25:501–531
- Steiger RH (1964) Dating of orogenic phases in the Central Alps by K-Ar ages of hornblende. *J Geophys Research* 69:5407–5421
- Steiger RH, Jäger E (1977) Subcommission on geochronology: Convention on the use of decay constants in geo- and cosmochronology. *Earth Planet Sci Lett* 36:359–362
- Stoekchert B, Jaeger E, Voll G (1986) K-Ar age determinations on phengites from the internal part of the Sesia Zone, Western Alps, Italy. *Contrib Mineral Petrol* 92:456–470
- Turner G (1966) The distribution of potassium and argon in chondrites. In: *Origin and distribution of the elements*. Ahrens LH (ed) Pergamon, Oxford New York 387–398
- Villa IM (1983) ⁴⁰Ar/³⁹Ar chronology of the Adamello gabbros, Southern Alps. *Mem Soc Geol It* 26:309–318
- York D (1969) Least square fitting of a straight line with correlated errors. *Earth Planet Sci Lett* 5:320–324
- Zeitler PK, Wijbrans JR (1986) A reassessment appraised: comment on “Hornblende K-Ar ages and the climax of tertiary metamorphism in the Lepontine Alps (south-central Switzerland): an old problem reassessed”. *Earth Planet Sci Lett* 76:390–392